CERN – EUROPEAN ORGANIZATION FOR NUCLEAR RESEARCH

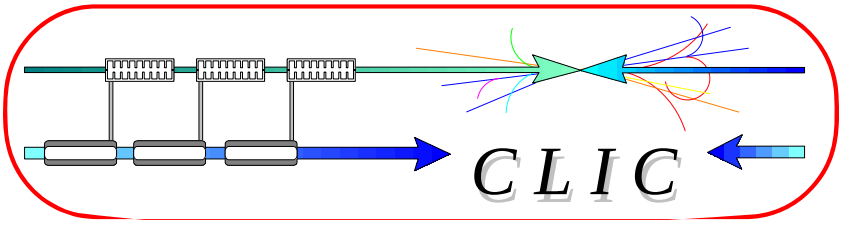

CLIC-Note-766

ESTIMATION OF THE RF CHARACTERISTICS OF ABSORBING MATERIALS IN BROAD RF FREQUENCY RANGES

R. Fandos, W. Wuensch

Keywords: absorbing material, silicon carbide, aluminum nitride, permittivity, loss tangent, RF measurements, Kramers & Kronig equations

CERN-OPEN-2008-019
30/06/2008

Abstract

Absorbing materials are very often used in RF applications. Their electromagnetic characteristics (relative permittivity ε_r, loss tangent $\tan\delta$ and conductivity σ) are needed in order to obtain a high-quality design of the absorbing pieces in the frequency range of interest. Unfortunately, suppliers often do not provide these quantities. A simple technique to determine them, based on the RF measurement of the disturbance created by the insertion of a piece of absorber in a waveguide, is presented in this note. Results for samples of two different materials, silicon carbide and aluminum nitride are presented. While the former has a negligible conductivity at the working frequencies, the conductivity of the latter has to be taken into account in order to obtain a meaningful estimation of ε_r and $\tan\delta$. The equations of Kramers & Kronig have been applied to the data as a cross check, confirming the results.

Geneva, Switzerland
June 2008

1. INTRODUCTION

Silicon carbide (SiC) has been commonly used in the CLIC prototypes, e.g., in damping loads for the accelerating structures [1], or also in absorbing parts in the CLIC WCM [2]. Aluminum nitride (AlN) has been considered as a candidate for the absorbers used in PETS [8]. The relative permittivity ε_r and loss tangent $\tan\delta$ in different frequency ranges of the material are needed to design the pieces. However, very few data exist in the literature, especially at CLIC frequencies.

The task of estimating these quantities was already addressed in [3] for a discrete number of frequency points. In this note, a modification to that setup is proposed, estimating the electromagnetic characteristics of the materials in continuous frequency ranges.

The method will be illustrated for measurements of SiC pieces at the frequency range from 29 to 33GHz and afterwards extended to other frequency ranges, and also to aluminum nitride samples.

The Kramers and Kronig equations have been applied to the results. The estimated electromagnetic characteristics accomplish the inter dependence that the equations establish, supporting the validity of the method.

2. DESCRIPTION OF THE METHOD

According to Maxwell equations, the relation between the rotational of the magnetic field $\vec{H}$ and the electric field $\vec{E}$ is as follows:

$$\nabla \times \vec{H} = (\sigma + j\omega\varepsilon)\vec{E} = j\omega\varepsilon_c\vec{E} \tag{2.1}$$

with ω the RF frequency, σ the conductivity of the material where the field propagates and ε its permittivity. For dielectrics, ε is assumed to be complex $\varepsilon = \varepsilon' + j\varepsilon''$. Grouping it with σ we define the complex permittivity ε_c

$$\varepsilon_c = \varepsilon_r(1 - j\tan\delta - j\frac{\sigma}{\omega\varepsilon_r}) \tag{2.2}$$

where ε_r is the real part of the permittivity, that is, $\varepsilon_r = \varepsilon'$, and $\tan\delta$ is the ratio between its imaginary and real parts, $\tan\delta = \varepsilon''/\varepsilon'$.

The value of the conductivity σ can be considered at constant from DC to about 100 GHz thus in our frequency range. For the studied SiC samples, σ has been measured by two different methods. The first one is the so-called 4 point method [7], the second one consists of establishing a fixed current across the entire length of the sample, and then measuring the potential difference between two points at known distance over the sample length.

The SiC conductivity has been found to be negligible thus $\varepsilon_c = \varepsilon_r(1 - j\tan\delta)$. As it will be described in section 6, the conductivity of aluminum nitride is not negligible, affecting the measurements and therefore has to be taken into account for the estimation of the permittivity.

With an electromagnetic simulation software, in our case HFSS, a set-up as shown in fig. 1 is studied. That same set-up is mechanically built and measured with a Network Analyzer. In HFSS, different ε_r and $\tan\delta$ are assumed for the SiC piece, obtaining a different transmission coefficient S21 for each option. The real and imaginary parts of the measured S21 are compared with those obtained by HFSS, choosing the combination of ε_r, $\tan\delta$ and σ that minimizes the difference.

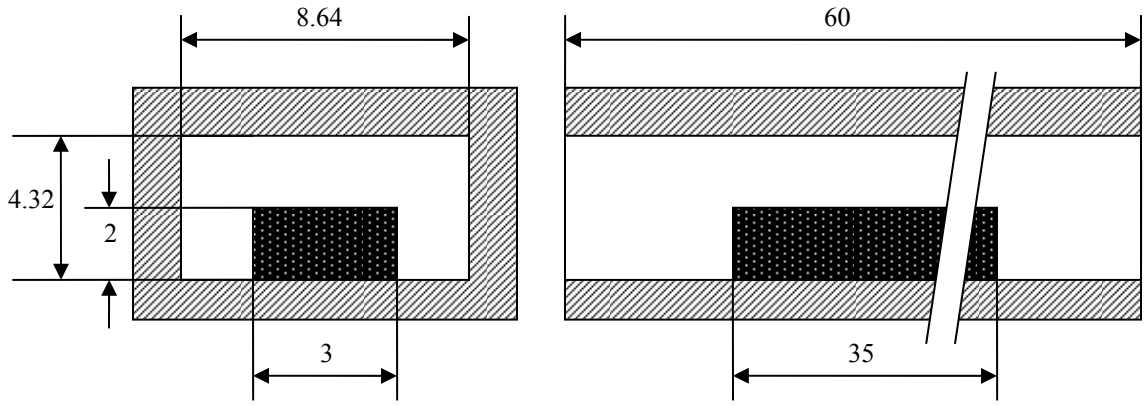

Figure 1: Experimental setup for the 29-33GHz frequency range. The waveguide is a standard WR34, the dimensions are in millimeters.

2.1 Precise positioning of the SiC. Tolerances

In order to assure that any change in the transmission coefficient is due to a change in ε_r and $\tan\delta$, the uncertainty in the geometry of the setting has to be minimized.

The position of the SiC into the waveguide has to be known precisely. For that, the piece of waveguide is cut in two parts, and a slot of known depth and the same width as the SiC piece is machined in one of them (see fig. 2). Thus, both the longitudinal and transverse positions of the SiC piece are fixed. Since small displacements may still occur, simulations including position tolerances of the SiC piece of up to 1mm have shown that the S21 parameter is insensitive to them.

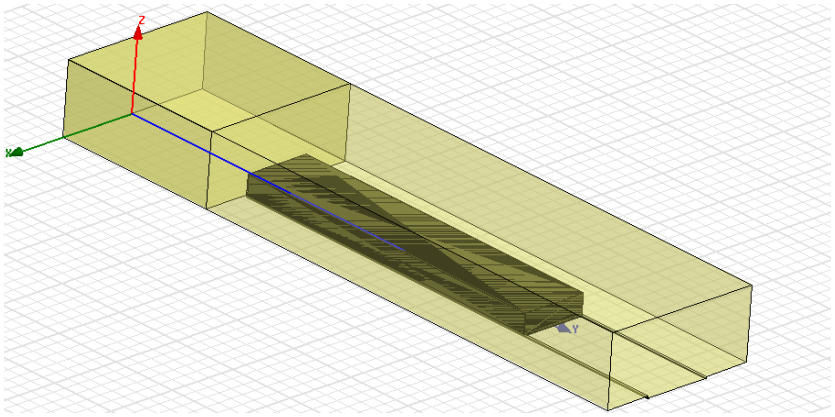

Figure 2: HFSS geometry for the 29-33GHz setup.

Moreover, measuring the S21 coefficient of the empty waveguide, the effect of the waveguide dimension tolerances can be neutralized, by correcting the waveguide length in the HFSS model so that its electrical length fits the one measured with the Network Analyzer.

2.2. Sensitivity of the measurement

In principle, the dimensions of the SiC piece can be freely chosen. However, if approximate values of ε_r and $\tan\delta$ are known, the geometry of the piece can be optimized such that the S21 coefficient is as sensitive as possible to permittivity changes.

A set of simulations sweeping the values of ε_r and $\tan\delta$ in ranges considered meaningful ($20<\varepsilon_r<40$, $0.2<\tan\delta<0.4$) have been performed for several SiC geometries. The results for two of those candidates are shown in fig. 3, but many more have been considered. The sensitivity of the S21 parameter to changes on the electromagnetic characteristics of the material is much higher for the bigger piece, that is, for the option shown on the right. On the other hand, the amplitudes of the curves are smaller (0.2 vs. 0.5 approx.). Thus, the relative effect of the noise and tolerances will be higher in that case. In general, the more sensitive S21 is to changes in the permittivity, the smaller its amplitude, and a compromise is necessary. The dimensions 35x3x2mm were finally chosen.

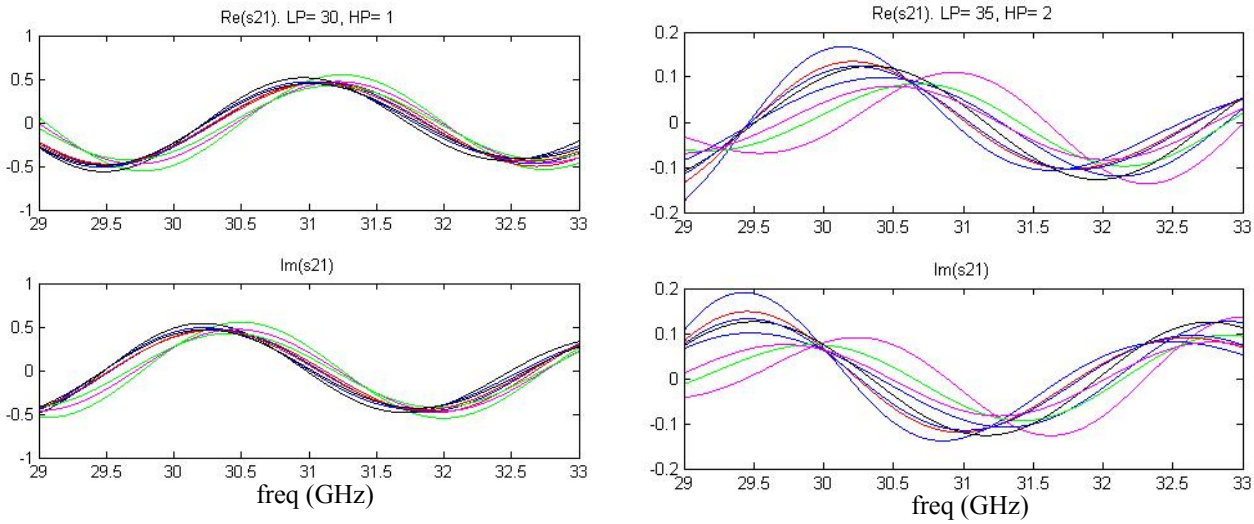

Figure 3: The picture on the left shows the real and imaginary parts of the S21 parameter for a piece of SiC of dimensions 30x3x1mm. Each color corresponding to a different ε_r (20,30,40) and $\tan\delta$ (0.2,0.3,0.4) combination, while the picture on the right corresponds to a piece of 35x3x2mm.

3. PERIMITTIVITY OF SIC IN THE 22-32GHZ FREQUENCY RANGE

The transmission coefficient measured with a Network Analyzer, for the geometry shown in fig. 1, is represented in fig. 4. As described in the previous section, the relative permittivity and loss tangent of the SiC piece are chosen such that the S21 parameters produced by HFSS fit the measured ones. For the 22-32 GHz frequency range and for this setting, the chosen ε_r and $\tan\delta$ as a function of frequency are shown in fig. 5.

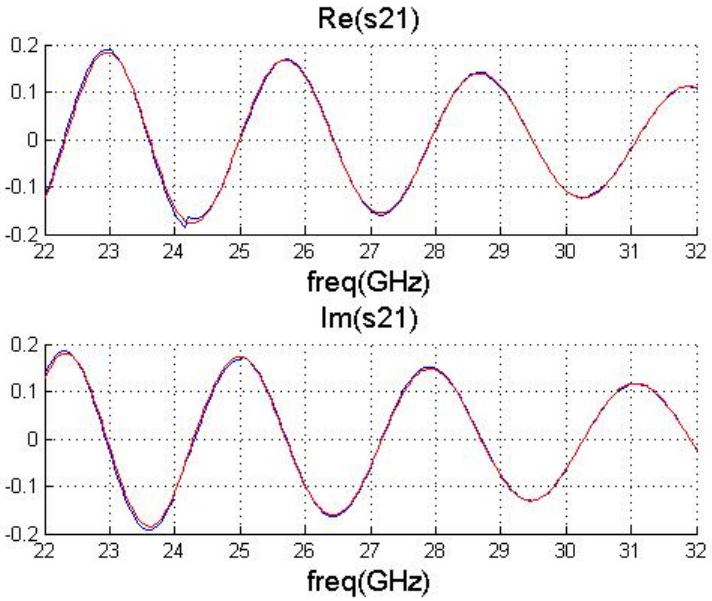

Figure 4: Real and imaginary parts of the transmission coefficient, S21. The curves in red are the Network analyzer measurements, while the blue curves correspond to the HFSS fit.

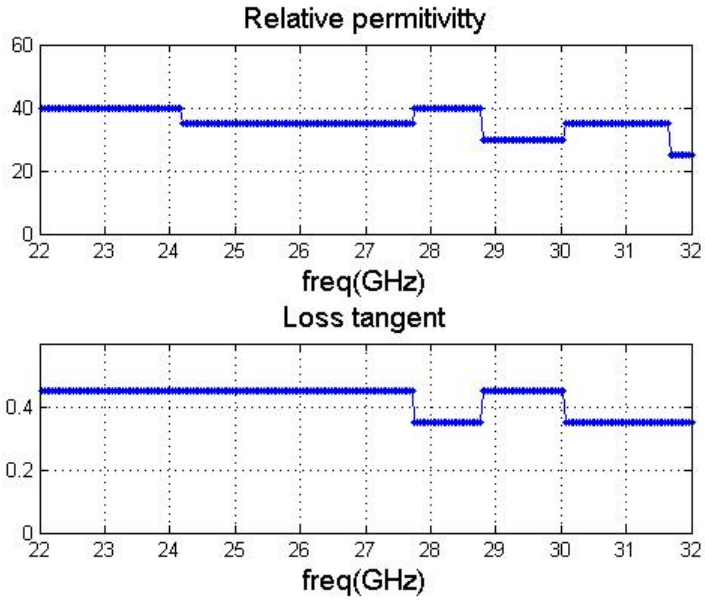

Figure 5: ε_r and tanδ that produce the Network Analyzer to HFFS S21 fit shown in fig 4.

4. EXTENSION OF THE METHOD TO OTHER FREQUENCY RANGES

The frequency ranges where to estimate the SiC permittivity are determined by the needs of the CLIC prototypes. The WCM design [3] needs measurements in the 3GHz region, at X-band and also around 20GHz. The damping of high order modes for the CLIC accelerating structures demands a band that reaches as high as possible in frequency. The limit for the maximum frequency has actually been set by the Network Analyzer characteristics.

4.1 Dimensions of the different settings

The flatness of ε_r and tanδ in frequency for the WR34 setting makes it reasonable to assume that they will not change abruptly (by orders of magnitude) in the neighboring frequency regions. Hence, instead of just scaling the previous setting to other waveguide standards, a sensitivity study (see sec. 2.2) has been performed for each of them. In table 1 the dimensions of the SiC pieces for the different settings are listed.

Frequency range (GHz)	Waveguide Standard	SiC length(mm)	SiC width(mm)	SiC height(mm)
36-46	WR22	15	3	1
30-37	WR28	15	3	1
7-13	WR90	48.4	9.6	3
2.6-4	WR284	210	16	10.5

Table 1: Silicon carbide piece dimensions for the different settings, corresponding to different frequency ranges.

4.2 Results

The electromagnetic characteristics of the SiC in the X-band frequency range are shown in fig. 6. One can observe that both ε_r and tanδ are very flat in this frequency range, presenting just a few presumably wrong points that correspond to the zero crossings of the real and imaginary parts of the transmission coefficient, and these can be filtered out (fig. 7).

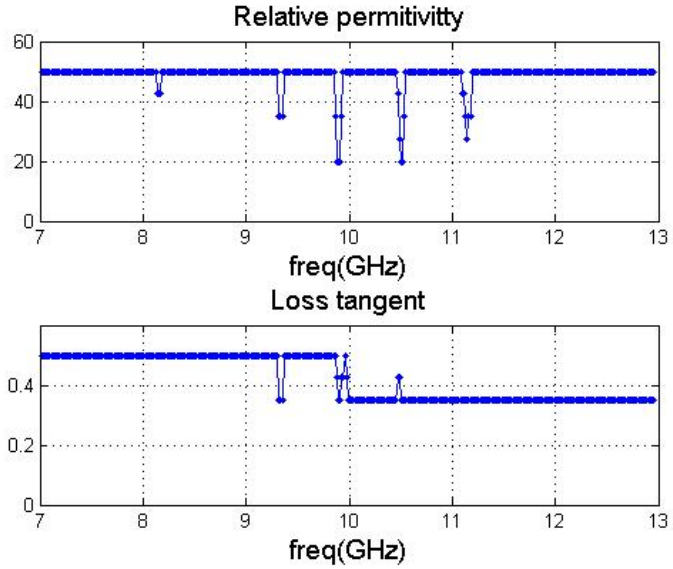

Figure 6: ε_r and tanδ of the SiC piece as a function of frequency in the range 7 to 13GHz.

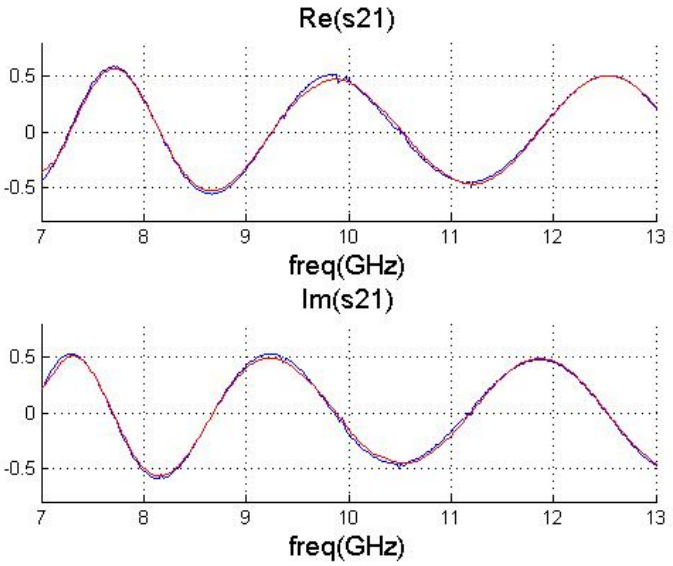

Figure 7: Real and imaginary parts of the transmission coefficient S21 in the X-band frequency range, for SiC samples. The curves in red are the Network analyzer measurements, while the blue curves correspond to the HFSS fit.

The experimental permittivity of SiC in the range 22-46GHz is shown in fig. 8. For that, three different measurement setups have been used, with standard WR34, WR28 and WR22 waveguides.

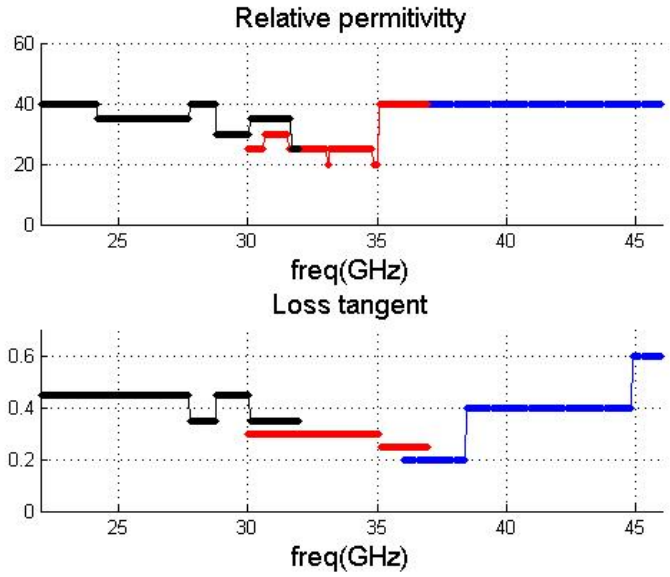

Figure 8: ε_r and tanδ as a function of frequency in the range 22 to 46GHz. The black curve corresponds to the WR34 setting, the red curve to the WR28 setting and the blue curve to the WR22 setting.

5. APPLICATION OF THE METHOD TO ALUMINUM NITRIDE

Aluminum nitride has been studied in the X-band frequency range, using the WR90 set-up described in 4.1. Unlike SiC, AlN has a non negligible conductivity when compared with tanδ in eq.2.2. Therefore its value, 100S/m for our samples, has been introduced in HFSS. The best fit between the S21 parameter measured with the Network Analyzer and the simulated one is found for ε_r =30 and tanδ=0.3 in the whole frequency range. The fit between the curves is shown in fig. 9.

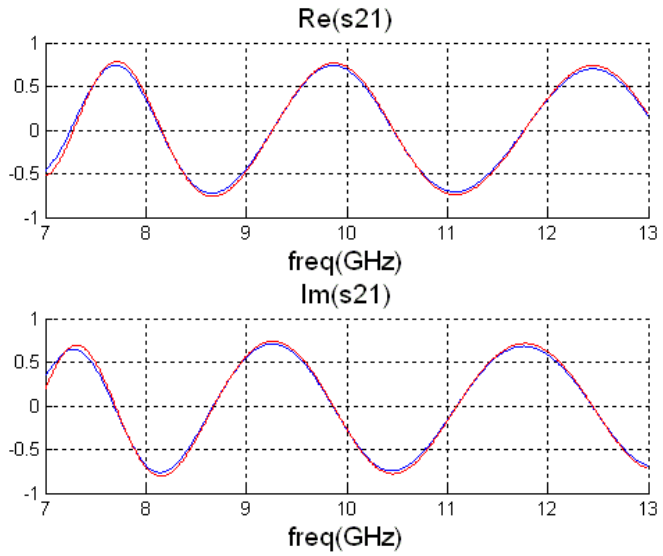

Figure 9: Real and imaginary parts of the transmission coefficient S21, in the X-band frequency range, for AlN samples. The curves in red are the Network analyzer measurements, while the blue curves correspond to the HFSS fit.

The same kind of AlN was investigated in [4], estimating its ε_r and tanδ using a completely different method, and obtaining exactly the same values.

6. CROSS CHECK WITH THE KRAMERS & KRONIG EQUATIONS.

The Kramers & Kronig equations [5] express an inter relation between the real ε' and the imaginary part ε'' of the permittivity, as a function of frequency:

$$\varepsilon'(\omega) - 1 = \frac{1}{\pi} P \int_0^{\infty} \frac{\varepsilon''(\omega)}{x - \omega} dx \qquad (6.1)$$

$$\varepsilon''(\omega) = -\frac{1}{\pi} P \int_0^{\infty} \frac{\varepsilon'(\omega)}{x - \omega} dx \qquad (6.2)$$

where P means the Cauchy principal value of the integral. Hence, from $\varepsilon'(\omega)$ it is possible to derive $\varepsilon''(\omega)$ and vice versa. In order to do so it is necessary to know these quantities in the whole frequency range, but we only have this information in finite ranges. However, using the fact that $\varepsilon''(\omega)$ is an odd function, equation 6.1 can be written as

$$\varepsilon'(\omega) - 1 = \frac{2}{\pi} P \int_0^{\infty} \frac{x\varepsilon''(\omega)}{x^2 - \omega^2} dx \qquad (6.3)$$

According to [4], it is possible to apply this equation even when $\varepsilon''(\omega)$ is only approximately known, as it is our case. The flatness of ε_r and $\tan\delta$ in the known frequency ranges makes reasonable to extrapolate these same values to neighboring regions. Furthermore, $\varepsilon''(\omega)$ decays at very high frequency, when the electrons cannot follow the changes in the field polarization [6]. The estimation of this frequency for our materials is beyond the purpose of this study.

The equations have been applied in the 20 to 45GHz frequency range for the SiC pieces. The absolute value of $\varepsilon'(\omega)$ that the equation predicts is dependent on the assumptions described in the paragraph above. However, the undulations that $\varepsilon'(\omega)$ has in that region are predicted by the equations, as can be observed in fig. 10.

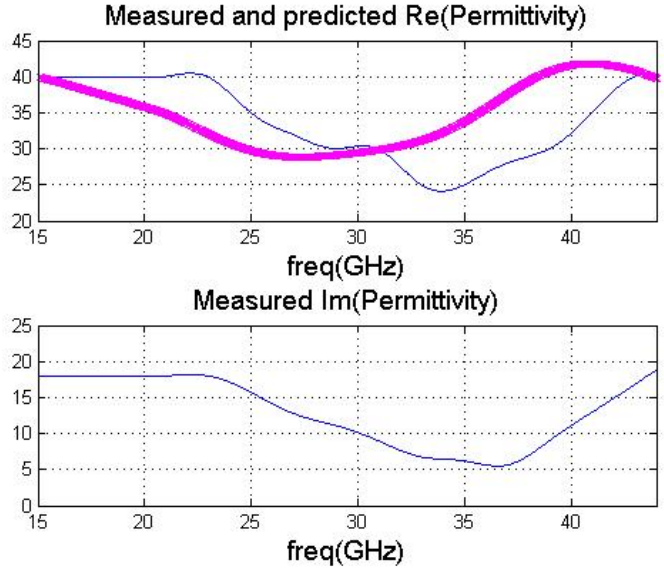

Figure 10: The blue curves show the values of ε' and ε'' estimated by HFSS. They have been extracted from the data plotted in fig. 8, sampling the curves at every integer gigahertz and applying afterwards a polynomial interpolation. ε' equals ε_r, while ε'' is the multiplication of ε_r and tanδ. The ε' predicted by the Kramers and Kronig equation (6.3) from ε'' is plotted in thick magenta, superimposed to the measured one.

8. REFERENCES

1. A. Grudiev, W. Wuensch, "Design of High Gradient Accelerating Structure for CLIC", *AIP Conf. Proc.* 807 (2006) pp.439-446

2. A. D'Elia, R. Fandos, L. Soby, "High Bandwidth Wall Current Monitor" EUROTeV Report, to be published

3. M. Luong, I. Wilson, W. Wuensch, "RF Loads for the CLIC Multibunch Structure", PAC, New York City, NY, USA, 29 Mar - 2 Apr 1999, pp.e-proc. 821

4. W. Main, S. Tantawi, J. Hamilton, "Measurements of the dielectric constant of lossy ceramics", International Journal of Electronics

5. E. M. Lifshitz and L. D. Landau, “Electrodynamics of Continuous Media”, Volume 8 (Course of Theoretical Physics)

6. J. D. Jackson, “Classical Electrodynamics”

7. L. B. Valdes, “Resistivity Measurements on Germanium for Transistors”, Proceedings of the IRE**,** Feb. 1954, Volume: 42, Issue: 2, pp. 420-427

8. I. Syratchev, “High RF Power Production for CLIC”, .CERN-AB-2007-059, CLIC-Note-720, 2007